

Cobalt(III) Halide Metal–Organic Frameworks Drive Catalytic Halogen Exchange

Tyler J. Azbell and Phillip J. Milner*



Cite This: *J. Am. Chem. Soc.* 2024, 146, 11164–11172



Read Online

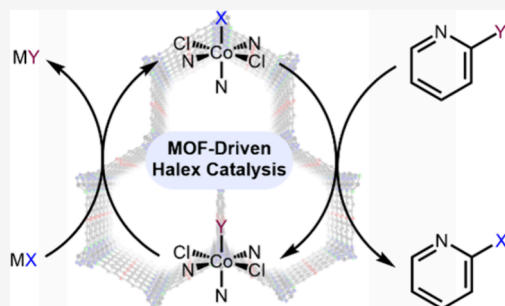
ACCESS |

Metrics & More

Article Recommendations

Supporting Information

ABSTRACT: The selective halogenation of complex (hetero)aromatic systems is a critical yet challenging transformation that is relevant to medicinal chemistry, agriculture, and biomedical imaging. However, current methods are limited by toxic reagents, expensive homogeneous second- and third-row transition metal catalysts, or poor substrate tolerance. Herein, we demonstrate that porous metal–organic frameworks (MOFs) containing terminal Co(III) halide sites represent a rare and general class of heterogeneous catalysts for the controlled installation of chlorine and fluorine centers into electron-deficient (hetero)aryl bromides using simple metal halide salts. Mechanistic studies support that these halogen exchange (halex) reactions proceed via redox-neutral nucleophilic aromatic substitution (S_NAr) at the Co(III) sites. The MOF-based halex catalysts are recyclable, enable green halogenation with minimal waste generation, and facilitate halex in a continuous flow. Our findings represent the first example of S_NAr catalysis using MOFs, expanding the lexicon of synthetic transformations enabled by these materials.



INTRODUCTION

Halogenated molecules are abundant in medicinal and agricultural chemistry, with fluorinated and chlorinated molecules representing >25% of active pharmaceuticals and >30% of agrochemicals.^{1–4} The replacement of hydrogen atoms in bioactive molecules with fluorine or chlorine generally leads to improved physiological effectiveness and bioavailability, termed the “magic fluorine” and “magic chlorine” effects, respectively.^{5–7} Among halogenated molecules, 2-haloheteroarenes are particularly common,^{8–12} exemplified by radiotracers for ¹⁸F positron emission tomography (PET),^{8,9} natural products,¹⁰ anticancer drugs,^{13,14} and painkillers (Figure 1a).^{10,15} Despite the ubiquity of halogens in bioactive molecules, their selective late-stage installation, especially with inexpensive metal halide salts, remains a major challenge.

Selective halogenation is inherently difficult due to the extreme reactivity of halogenating agents such as F₂ and Cl₂, both of which are impractically hazardous for common laboratory use.^{16–18} As an alternative, the Balz–Schiemann reaction—which involves the thermolysis of potentially explosive tetrafluoroborate diazonium salts—requires harsh conditions and displays modest heterocycle compatibility.^{19,20} The most common method for incorporating halogens into heteroarenes is via nucleophilic halogen exchange (halex), a nucleophilic aromatic substitution (S_NAr) reaction in which an existing halogen (e.g., Br) is replaced with the desired halogen (e.g., Cl, F).^{21,22} Traditionally, this process requires the use of high reaction temperatures (>200 °C) and/or complex phase-transfer catalysts due to the poor solubility of simple metal

halide salts such as KF.^{23,24} More complex halex reagents consist of soluble tetraalkylammonium^{25–28} or acyl imidazolium salts,²⁹ stoichiometric reagents that generate soluble and/or toxic organic byproducts that can be challenging to separate from the desired product (Figure 1b).^{28–30} Catalytic halex has been achieved using a number of second- and third-row transition metal reagents;^{31–35} however, examples of halex mediated by more abundant first-row transition metal catalysts remain rare.^{36–39} This is likely because all examples of transition-metal-catalyzed halex reported to date proceed through a cross-coupling mechanism, with a halide exchange step (rather than transmetalation) prior to sluggish reductive elimination to form the aryl halide product.^{33,40} This is in contrast to the outer-sphere halide transfer mechanism through which simple metal halide salts (e.g., KF, CsF) mediate halex.^{24,41} Notably, examples of heterogeneous and recyclable catalysts for halex remain limited to ill-defined materials such as Ni metal and Pd/C.^{36,42}

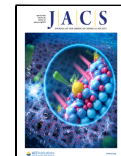
Highly nucleophilic halide sites are critical to halex. Terminal metal halide (M–X) species potentially offer the nucleophilicity necessary to facilitate catalytic halogen exchange, but they require bulky ligand systems to prevent

Received: December 8, 2023

Revised: March 20, 2024

Accepted: March 23, 2024

Published: April 12, 2024



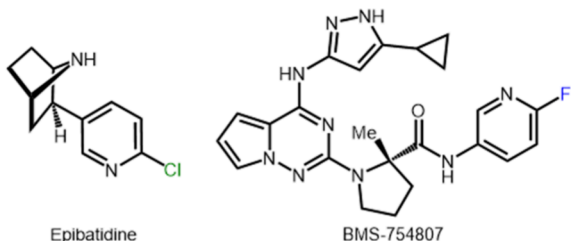
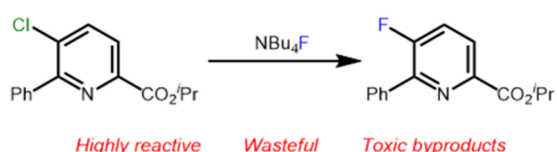
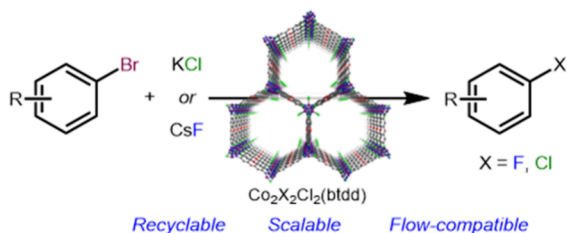
a 2-haloheteroarenes:**b** Molecular halex reagents:**c** MOF-driven halex (this work):

Figure 1. (a) Examples of 2-halopyridines present in a natural product (epibatidine)¹⁰ and a pharmaceutical (BMS-754807).¹³ (b) Representative example of halex by soluble fluoride reagents.^{25,28} (c) Halex driven by $\text{Co}_2\text{X}_2\text{Cl}_2(\text{btdd})$. Purple, gray, blue, red, and green spheres correspond to cobalt, carbon, nitrogen, oxygen, and chlorine, respectively.

μ -dimerization in solution.^{33,40,43} While this dimerization is difficult to combat in molecular systems, a solid-state platform bearing discrete terminal M–X sites at structurally integral points would prevent dimerization entirely. Indeed, metal–organic frameworks (MOFs), crystalline materials constructed from organic linkers and inorganic nodes, can possess terminal M–X centers.^{44–47} For example, the framework $\text{Co}_2\text{Cl}_2(\text{btdd})$ ($\text{btdd}^{2-} = \text{bis}(1\text{-}H\text{-}1,2,3\text{-triazolo}[4,5-*b*],[4',5'-*i*]\text{-dibenz}[1,4]\text{-dioxin})$)⁴⁸ can be oxidized by the elemental halogens Cl_2 and Br_2 to afford the frameworks $\text{Co}_2\text{Cl}_4(\text{btdd})$ and $\text{Co}_2\text{Br}_2\text{Cl}_2(\text{btdd})$, respectively, which bear terminal Co(III)–X centers pointing into their pores (X_T, Figure 2a).⁴⁷ Moreover, MOFs offer inherent recyclability and scalability over homogeneous catalysts and compatibility with application in continuous flow.⁴⁹

Herein, we demonstrate that $\text{Co}_2\text{X}_2\text{Cl}_2(\text{btdd})$ (X = F, Cl, Br, I) MOFs containing terminal M–X sites catalyze the chlorination and fluorination of a range of electron-deficient (hetero)arenes using simple metal halide salts (Figure 1c). These frameworks are among the first heterogeneous and recyclable catalysts for halex⁵⁰ and the first MOF-based catalysts for S_NAr reactions. The catalytic transformations can be readily scaled (to 1.0 g) in batch or continuous flow, providing a green alternative to the current approaches. Overall, this work establishes a transformation previously unexplored using MOF catalysts and facilitates the development of a range of nucleophilic reactions, including those prohibited using molecular catalysts.

RESULTS AND DISCUSSION

MOF Synthesis. Assessment of the suitability of $\text{Co}_2\text{X}_2\text{Cl}_2(\text{btdd})$ frameworks as halex catalysts requires a method to prepare these frameworks reliably on a gram scale. By merging previously reported high-concentration and ionothermal methods,^{46,51} we achieved the first high-concentration solvothermal synthesis of $\text{Co}_2\text{Cl}_2(\text{btdd})$, enabling its rapid synthesis on a gram scale (Supporting Information Section 3). Simply combining the H_2btdd linker, $\text{CoCl}_2\cdot 6\text{H}_2\text{O}$, *N,N*-dimethylformamide (DMF), and concentrated HCl together at a linker concentration of 1.0 M in a Teflon autoclave at 160 °C for 16 h affords $\text{Co}_2\text{Cl}_2(\text{btdd})$ in 60% yield. The powder X-ray diffraction (PXRD) pattern of $\text{Co}_2\text{Cl}_2(\text{btdd})$ prepared under high-concentration conditions is in good agreement with the simulated pattern based on the expected structure (Figures S3 and S4).⁴⁸ The prepared MOF possesses a record-high 77 K N_2 Brunauer–Emmett–Teller (BET) surface area ($2532 \pm 119 \text{ m}^2/\text{g}$) after soaking in organic solvents to remove soluble impurities and activation under vacuum (Figure S5). Scanning electron microscopy (SEM), combustion elemental analysis, and thermogravimetric analysis (TGA) further support the successful synthesis of high-quality $\text{Co}_2\text{Cl}_2(\text{btdd})$ under these conditions (Figures S8 and S9, Table S1).⁴⁶

Activated $\text{Co}_2\text{Cl}_2(\text{btdd})$ was employed to prepare the halogenated Co(III) analogues via one-electron oxidation with electrophilic halogen sources (Figure 2). Following methods reported in the literature,⁴⁷ the chlorinated framework $\text{Co}_2\text{Cl}_4(\text{btdd})$ was prepared via oxidative halogenation using Cl_2 or PhICl_2 (Figure 2a). The brominated framework was similarly synthesized by using a modified vapor diffusion method with Br_2 , affording $\text{Co}_2\text{Br}_2\text{Cl}_2(\text{btdd})$ (Figure 2a). The prepared samples of $\text{Co}_2\text{Cl}_4(\text{btdd})$ and $\text{Co}_2\text{Br}_2\text{Cl}_2(\text{btdd})$ demonstrate comparable crystallinities and BET surface areas to those reported in the literature (Figure 2c,d and Figures S17–S19).⁴⁷ Inspired by these results, we sought to access the entire halogenated series of $\text{Co}_2\text{X}_2\text{Cl}_2(\text{btdd})$ MOFs by preparing novel fluorinated and iodinated frameworks. An analogous hypervalent iodine oxidant to PhICl_2 , PhIF_2 ,⁵² was employed to access $\text{Co}_2\text{F}_2\text{Cl}_2(\text{btdd})$ for the first time (Figure 2a). Previous attempts to prepare the Co(III)–I material with solution-state iodination were unsuccessful;⁴⁷ however, heating solid I₂ at 60 °C was found to yield $\text{Co}_2\text{I}_2\text{Cl}_2(\text{btdd})$ via vapor diffusion.

All halogenated Co(III) frameworks retain their crystallinity by PXRD (Figure 2c) and demonstrate reasonably attenuated surface areas compared to $\text{Co}_2\text{Cl}_2(\text{btdd})$ (Figure 2d and Figures S17–S19). Characterization by combustion elemental analysis, X-ray photoelectron spectroscopy (XPS), and energy-dispersive X-ray spectroscopy (EDS) further supports the successful oxidative halogenation of all four MOFs (see Supporting Information Section 4 for details). In particular, EDS images confirm the uniform distribution of the appropriate halogens throughout the MOF crystallites (Figures S23–S27 and Tables S3–S7). Among these techniques, combustion elemental analysis was found to yield the most reliable data for quantifying the halogen content of MOFs (Tables S1 and S12–S16). With the exception of $\text{Co}_2\text{F}_2\text{Cl}_2(\text{btdd})$, which contains F atoms that are difficult to detect via combustion analysis,⁵³ the halogen contents of all Co(III) MOFs were found to be within ~4% of the theoretical values. Notably, all four MOFs were also found to retain

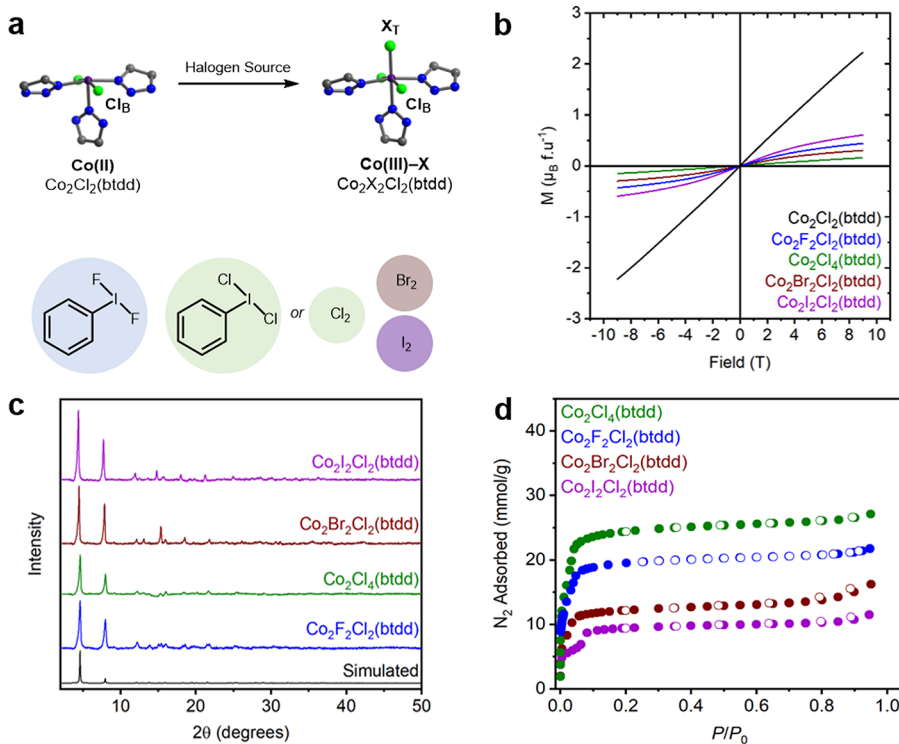


Figure 2. (a) Oxidation of $\text{Co}_2\text{Cl}_2(\text{btdd})$ to $\text{Co}_2\text{X}_2\text{Cl}_2(\text{btdd})$ with the corresponding halogen sources. Cl_B represents the bridging chlorides of the secondary building unit, while X_T represents terminal halogens appended to the metal site, pointing into the pore. (b) SQUID magnetometry moment vs field (MvH) measurements of $\text{Co}_2\text{Cl}_2(\text{btdd})$ (black), $\text{Co}_2\text{F}_2\text{Cl}_2(\text{btdd})$ (blue), $\text{Co}_2\text{Cl}_4(\text{btdd})$ (green), $\text{Co}_2\text{Br}_2\text{Cl}_2(\text{btdd})$ (brown), and $\text{Co}_2\text{I}_2\text{Cl}_2(\text{btdd})$ (purple). (c) PXRD patterns of $\text{Co}_2\text{F}_2\text{Cl}_2(\text{btdd})$ (blue), $\text{Co}_2\text{Cl}_4(\text{btdd})$ (green), $\text{Co}_2\text{Br}_2\text{Cl}_2(\text{btdd})$ (brown), and $\text{Co}_2\text{I}_2\text{Cl}_2(\text{btdd})$ (purple). The simulated pattern based on the SCXRD structure of $\text{Mn}_2\text{Cl}_2(\text{btdd})$ is included for reference. (d) N_2 adsorption (filled circles) and desorption (open circles) isotherms of activated $\text{Co}_2\text{F}_2\text{Cl}_2(\text{btdd})$ (blue), $\text{Co}_2\text{Cl}_4(\text{btdd})$ (green), $\text{Co}_2\text{Br}_2\text{Cl}_2(\text{btdd})$ (brown), and $\text{Co}_2\text{I}_2\text{Cl}_2(\text{btdd})$ (purple). Purple, gray, blue, and green spheres correspond to cobalt, carbon, nitrogen, and chlorine, respectively.

significant amounts of Cl due to the preservation of the bridging μ -Cl sites in the framework (Cl_B , Figure 2a; see below for further discussion). As expected, the density functional theory-calculated pore sizes of the MOFs decrease as larger anions are incorporated, contracting from ~ 19 \AA in $\text{Co}_2\text{F}_2\text{Cl}_2(\text{btdd})$ to ~ 8 \AA in $\text{Co}_2\text{I}_2\text{Cl}_2(\text{btdd})$ (Figure S20). Last, Pawley refinements of the PXRD patterns of $\text{Co}_2\text{Cl}_2(\text{btdd})$ (Figure S4) and the halogenated MOFs (Figure S18) support that all of the MOFs are isostructural, but the latter are slightly contracted in a and c , as would be expected due to the shorter metal–ligand distances upon metal oxidation (Table S2).

Superconducting quantum interference device (SQUID) magnetometry was used to quantify the extent of Co(III) incorporation in the oxidized MOFs (Figure 2b). Isothermal moment vs field (MvH) measurements were performed at 5 K, sweeping from -9 to 9 T and back. The parent-activated Co(II) framework exhibits a linear response to the changing magnetic field, consistent with previous reports for this MOF (Figures S12 and S13)⁴⁷ describing a putative d^7 metal in a square-pyramidal ligand field ($S = 3/2$), with a maximum magnetization value of $2.28 \mu_B$ per formula unit. This value was used as the reference point for a 100% Co(II) material when calculating the percentage of residual Co(II) centers in the oxidized samples.⁴⁷ All samples of MOF collected after oxidation exhibit attenuated maximum magnetization values and S-shaped-curve profiles compared to those of the parent $\text{Co}_2\text{Cl}_2(\text{btdd})$, indicative of a predominantly low-spin octahedral Co(III) d^6 material ($S = 0$) diluted with some percentage

of residual, paramagnetic Co(II) sites. In all cases, the halogenated MOFs exhibit $>80\%$ conversion of the Co(II) sites to Co(III)–X centers (Figure 2b and Figure S53). High-resolution Co XPS further supports the assignment of the four oxidized MOFs as mixed Co(II)/Co(III) materials (Figures S30, S36, S42, S47, and S51).

The bridging μ -Cl ligands of $\text{M}_2\text{Cl}_2(\text{btdd})$ ($\text{M} = \text{Co, Ni}$) frameworks have been shown to be labile toward halogen exchange without framework decomposition.^{54–56} This attribute is required for the terminal M–X sites, as well, to facilitate halex catalysis. In order to assess whether these terminal M–X sites can be exchanged, $\text{Co}_2\text{Br}_2\text{Cl}_2(\text{btdd})$ was soaked in a 0.1 M solution of tetrabutylammonium fluoride (TBAF) in tetrahydrofuran (THF). This procedure affords a sample of $\text{Co}_2\text{F}_2\text{Cl}_2(\text{btdd})$ with a comparable PXRD pattern and BET surface area to the material synthesized from $\text{Co}_2\text{Cl}_2(\text{btdd})$ using PhIF_2 (Figures S17 and S19). Notably, this anion-exchanged framework does not contain residual tetraalkylammonium cations, as determined via a lack of alkyl stretches in its infrared (IR) spectrum (Figure S22). Further, EDS confirms the full exchange of terminal Br ions for F ions while also retaining some of the bridging μ -Cl ligands, although quantifying the degree of exchange between the bridging anions remains difficult (Figure S24 and Table S4). This measurement confirms that the terminal M–X sites in $\text{Co}_2\text{X}_2\text{Cl}_2(\text{btdd})$ readily undergo halogen exchange.

Reaction Development. We hypothesized that the terminal Co(III)–X sites in the $\text{Co}_2\text{X}_2\text{Cl}_2(\text{btdd})$ MOFs should function as reactive nucleophilic sites capable of undergoing

halex with suitable electrophiles (Figure 3). Indeed, treatment of 2-bromopyridine (2-BrPy) with a stoichiometric amount of

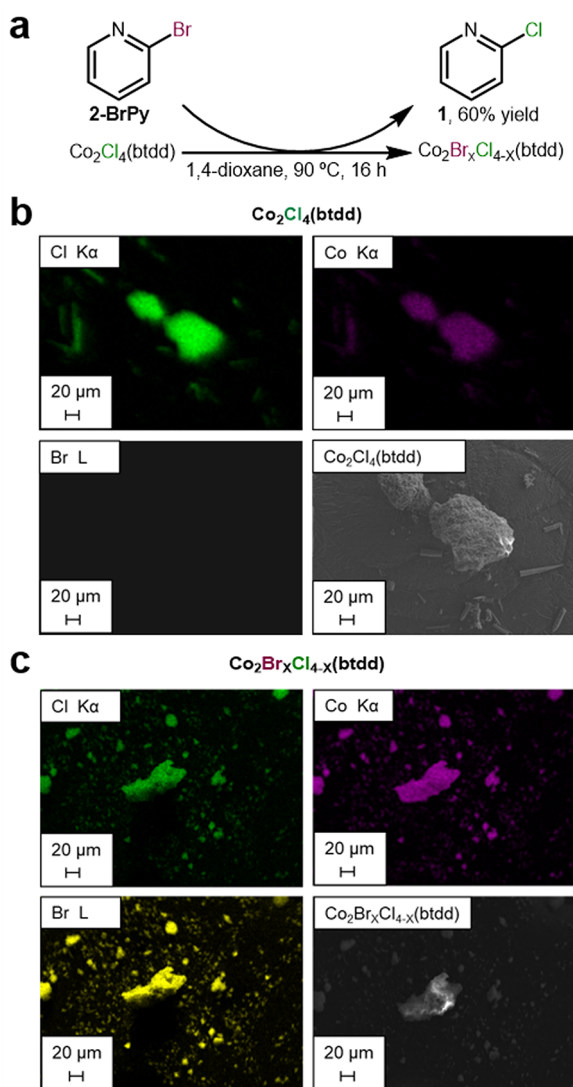


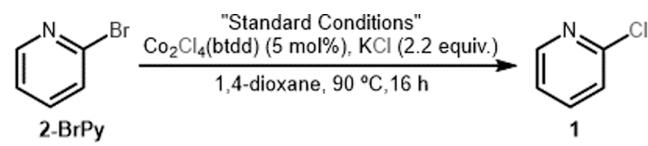
Figure 3. (a) Stoichiometric halex of 2-bromopyridine with $\text{Co}_2\text{Cl}_4(\text{btdd})$. (b) EDS elemental maps (top, bottom left) and SEM image (bottom right) of $\text{Co}_2\text{Cl}_4(\text{btdd})$. (c) EDS elemental maps (top, bottom left) and SEM image (bottom right) of $\text{Co}_2\text{Br}_x\text{Cl}_{4-x}(\text{btdd})$ recovered from the stoichiometric reaction in (a). The Br:Cl ratio was determined to be 2.3:1 (Table S19).

$\text{Co}_2\text{Cl}_4(\text{btdd})$ in 1,4-dioxane at 90 °C results in halogen exchange: 2-chloropyridine (1) was detected in 60% yield (Figure 3a), and Br was incorporated into the framework to produce $\text{Co}_2\text{Br}_x\text{Cl}_{4-x}(\text{btdd})$, as confirmed by EDS before and after the stoichiometric halex reaction (Figure 3b,c, Figure S57, and Table S19). XPS further supports the idea that the partially halogen-exchanged MOF contains both Br and Cl (Figures S58 and S59, Table S20). Notably, the resulting brominated framework was washed thoroughly with organic solvents to ensure that residual organics were removed from the MOF; thus, only Br covalently appended to the metal center of the framework should be detected with this technique. The partially halogen-exchanged MOF $\text{Co}_2\text{Br}_x\text{Cl}_{4-x}(\text{btdd})$ collected from this stoichiometric reaction retains its crystallinity, as confirmed by PXRD (Figure S60).

Additionally, the halex process is redox-neutral, indicated by the framework demonstrating nearly identical MvH field responses before and after the reaction (Figure S62). Lastly, graphite furnace atomic adsorption spectroscopy (GFAAS) of the filtrate confirmed that metal leaching does not occur during this stoichiometric reaction, supporting the idea that the reaction is not mediated by soluble Co salts (Table S21). Overall, this stoichiometric reaction supports that the terminal Co(III)–Cl sites in $\text{Co}_2\text{Cl}_4(\text{btdd})$ are nucleophilic enough to undergo halex with activated (hetero)aryl bromides. This is the first time that nucleophilic exchange has been demonstrated using isolated M–X sites in MOFs.

Inspired by this finding, we set out to render this reaction catalytic by using KCl as an inexpensive, exogenous halide source, necessary for turning the MOF over after the initial halogen exchange with the (hetero)aryl bromide (Table 1; see

Table 1. Optimization of Catalytic Chlorination



Entry	Deviation from Std.	GC Yield
1	None	50%
2	25 °C	10%
3	No KCl	3%
4	1.1 equiv. KCl	36%
5	4.4 equiv. KCl	52%
6	No MOF	0%
7	$\text{Co}_2\text{Cl}_2(\text{btdd})$ instead of $\text{Co}_2\text{Cl}_4(\text{btdd})$	0%
8	$\text{CoCl}_2 \cdot 6\text{H}_2\text{O}$ instead of $\text{Co}_2\text{Cl}_4(\text{btdd})$	0%
9	$[\text{Co}(\text{NH}_3)_5\text{Cl}]\text{Cl}_2$ instead of $\text{Co}_2\text{Cl}_4(\text{btdd})$	0%
10	$[\text{Co}(\text{NH}_3)_6]\text{Cl}_3$ instead of $\text{Co}_2\text{Cl}_4(\text{btdd})$	0%
11	Filter reaction mixture after 30 min	3%
12	$\text{Co}_2\text{Br}_2\text{Cl}_2(\text{btdd})$ instead of $\text{Co}_2\text{Cl}_4(\text{btdd})$	50%

Table 21 for optimization details). By dropping the loading of $\text{Co}_2\text{Cl}_4(\text{btdd})$ to 5 mol % and employing a slight excess of KCl (2.2 equiv), 1 was obtained in comparable yield (50%) to the stoichiometric reaction (entry 1, Table 1). The modest yield of this reaction is likely because it is reversible, as the bromination of 2-chloropyridine using KBr could be driven using the corresponding brominated MOF (Supporting Information Section 5). Control experiments confirm that heat, exogenous chloride, and chlorinated MOF are all necessary for the reaction to proceed in good yield (entries 2–5, Table 1). Critically, attempts to drive the reaction using the Co(II) MOF $\text{Co}_2\text{Cl}_2(\text{btdd})$ were unsuccessful (entry 7, Table 1), which serves as evidence that the terminal Co(III)–Cl sites in $\text{Co}_2\text{Cl}_4(\text{btdd})$ —and not the presumably less-labile bridging Cl sites—are vital to halex. Similarly, $\text{CoCl}_2 \cdot 6\text{H}_2\text{O}$ and the simple Co(III) salts $[\text{Co}(\text{NH}_3)_5\text{Cl}]\text{Cl}_2$ and $[\text{Co}(\text{NH}_3)_6]\text{Cl}_3$ are ineffective catalysts (entries 8–10, Table 1). A heterogeneous control test, in which the reaction was allowed to proceed for

Table 2. Scope of $\text{Co}_2\text{Cl}_4(\text{btdd})$ -Catalyzed Chlorination (Isolated Yield Unless Otherwise Noted)

$(\text{Het})\text{Ar}-\text{Br}$	KCl (2.2 equiv.) $\text{Co}_2\text{Cl}_4(\text{btdd})$ (5 mol%) 1,4-dioxane, 90 °C, 16 h	$(\text{Het})\text{Ar}-\text{Cl}$
1, 55%		
2, 50%		
3a, R = H, 32%		
3b, R = Cbz, 63%		
3c, R = Ts, 67%		
4a, R = H, 39%		
4b, R = Ts, 77%		
5a, R = CO2Me, 54%		
5b, R = CN, 47%		
5c, R = NO2, 38%		
6, 18%		
7, 68%		
8, 82%		
9, 58%		
10, 33%		
11, 47%		
12, 31%^a		
13a, R = H, 44%		
13b, R = Cbz, 66%		
14, 63%		
15a, R = H, 45%		
15b, R = Ts, 91%		
16, 43%		
3-CIPy, 0%		

^aGC yield relative to an internal standard of dodecane; product is contaminated with the dichlorinated product 2,5-dichloropyrazine.

30 min before filtering to remove the MOF, resulted in a minimal product (3% yield). These control experiments support that the unique coordination environment of the Co(III)-Cl sites within $\text{Co}_2\text{Cl}_4(\text{btdd})$ is key for effective catalysis, producing $\text{Co}_2\text{Br}_X\text{Cl}_{4-X}(\text{btdd})$ that can be turned over by the exogenous KCl in solution (Figure 4).

With the optimized conditions in hand, we explored the scope of the $\text{Co}_2\text{Cl}_4(\text{btdd})$ -catalyzed chlorination of electron-deficient (hetero)aryl bromides (Table 3). A range of (hetero)aryl bromides, including 5- and 6-membered hetero-

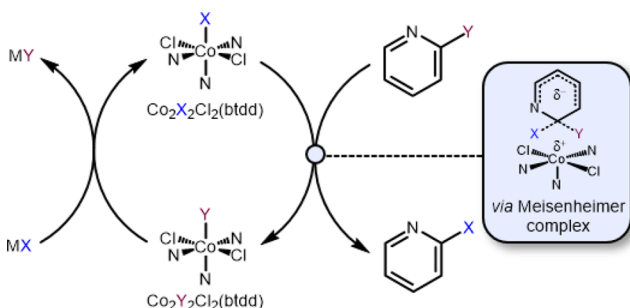


Figure 4. Proposed mechanism of MOF-driven halex catalysis.

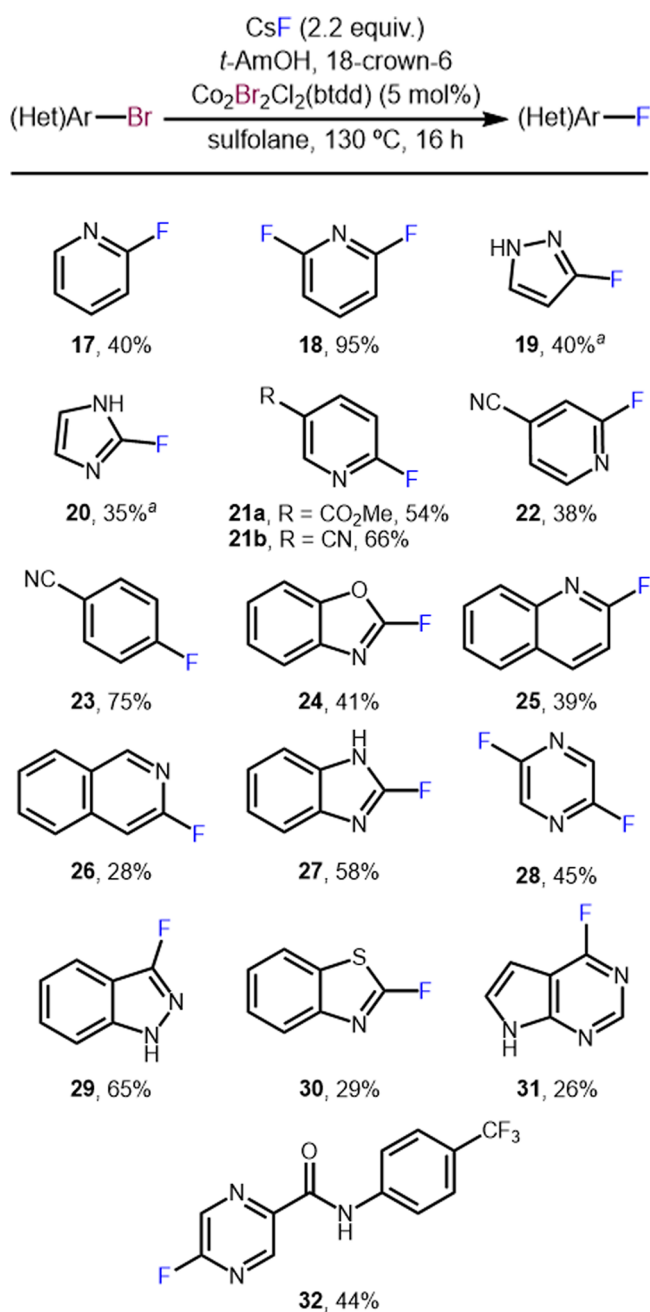
arenes, react smoothly to afford the corresponding (hetero)aryl chlorides. Notably, reports of halex reactions with 5-membered heterocycles are limited, supporting that the enhanced nucleophilicity of the halide sites within the MOF enables otherwise difficult transformations under mild conditions.^{57–59}

In most cases, the free N-H five-membered heteroaryl bromides can be used directly to produce the desired products in modest yields (3a, 4a, 11, 13a, 15a), although the use of N-protecting groups generally leads to higher yields. The reaction tolerates a range of electrophilic functional groups commonly found in drug-like molecules, including esters (5a), nitriles (5b, 7), nitroaromatics (5c), and amides (16). Notably, electron-deficient aryl bromides are also suitable substrates (7), further supporting the notion that these reactions likely proceed via an $S_N\text{Ar}$ mechanism. Background reactions in the absence of $\text{Co}_2\text{Cl}_4(\text{btdd})$ were conducted with five substrates; the expected products were observed in $\leq 1\%$ yield in all cases (Table S24). Notably, a neutral substrate, 4-bromobiphenyl, and an electron-rich substrate, 4-bromoanisole, showed no reactivity under the halex chlorination conditions, consistent with an $S_N\text{Ar}$ mechanism (Supporting Information Section 5).

We next evaluated whether Co(III)-X MOFs can catalyze other halex reactions, specifically the fluorination of (hetero)aryl bromides with simple metal fluoride salts (see Table S23 for optimization details). Initial studies using $\text{Co}_2\text{F}_2\text{Cl}_2(\text{btdd})$ resulted in poor yields and framework decomposition (entry 17, Table S23). This is likely due to the fragility of the isolated Co(III)-F framework, which demonstrates lower crystallinity compared to those of the other halogenated frameworks prepared herein (Figure 2c). However, with the knowledge that $\text{Co}_2\text{F}_2\text{Cl}_2(\text{btdd})$ can be prepared via anion exchange (see discussion above), this decomposition issue could be circumvented by generating Co(III)-F sites *in situ* from $\text{Co}_2\text{Br}_2\text{Cl}_2(\text{btdd})$ (see Table S23 for optimization details). Further modifications had to be made in order to accommodate the insolubility of metal fluoride salts, including the switch to the high-boiling solvent sulfolane and the addition of *tert*-amyl alcohol (*t*-AmOH) and 18-crown-6, both of which are reported to improve the solubility of metal fluoride salts (Table S23).⁶⁰ Notably, $\text{Co}_2\text{Cl}_2(\text{btdd})$ does not catalyze this transformation (Table S23), further supporting the importance of the terminal M-X sites for halex catalysis.

Using these optimized conditions, we explored the scope of the MOF-catalyzed fluorination of electron-deficient (hetero)aryl bromides (Table 3). Despite the independent importance of 5-membered heteroarenes and fluoroarenes in the pharmaceutical industry, 5-membered heteroaryl fluorides remain understudied due to a lack of methods available for their synthesis.⁶¹ Fluorination of the free N-H 5-membered heteroaryl bromides 19 and 20 proceed in comparable yields

Table 3. Scope of $\text{Co}_2\text{Br}_2\text{Cl}_2(\text{btdd})$ -Catalyzed Fluorination (Isolated Yield Unless Otherwise Noted)^a



^a¹⁹F NMR yield relative to an internal standard of fluorobenzene.

to the corresponding chlorination reactions. The reaction also tolerates a range of pharmaceutically relevant functional groups, including esters (21a), nitriles (21b), and amides (32). The relatively mild conditions combined with the enhanced nucleophilicity of the halide sites in the MOF afford access to a number of heteroaryl fluorides that have not previously been prepared via halex (27, 29, 30, 31).^{62–65} A lack of $\text{S}_{\text{N}}\text{Ar}$ reactivity was observed when 4-bromobiphenyl and 4-bromoanisole were subjected to the fluorination conditions, confirming the need for electron-deficient substrates to facilitate halex (Supporting Information Section 5). Background reactions in the absence of $\text{Co}_2\text{Br}_2\text{Cl}_2(\text{btdd})$ were run on five substrates (Table S25), all of which proceeded in

≤3% yield. These findings are the first report of a Co species, regardless of the oxidation state or solubility, mediating fluorination via halex.

Further mechanistic investigations were conducted to validate the proposed catalytic cycle (Figure 4). Halex reactions—and $\text{S}_{\text{N}}\text{Ar}$ reactions in general—typically proceed through a reactive intermediate known as a Meisenheimer or σ -complex (Figure 4).⁶⁶ To probe the mechanism of MOF-catalyzed halex, 3-bromopyridine, a classically $\text{S}_{\text{N}}\text{Ar}$ -inactive substrate,²⁶ was subjected to the optimized chlorination conditions. Gratifyingly, no chlorinated product (3-ClPy) was observed (Table 2). Because the $\text{Co}_2\text{Br}_X\text{Cl}_{4-X}(\text{btdd})$ MOF generated from the catalytic chlorination reaction contains Co(III)–Br centers that should be regenerated to Co(III)–Cl centers by exogenous KCl, $\text{Co}_2\text{Br}_2\text{Cl}_2(\text{btdd})$ should be able to drive catalytic chlorination reactions similarly to its fully chlorinated counterpart. Indeed, the chlorination of 2-BrPy to 1 with $\text{Co}_2\text{Br}_2\text{Cl}_2(\text{btdd})$ proceeded with comparable yield (50%, entry 12, Table 1) to that performed with $\text{Co}_2\text{Cl}_4(\text{btdd})$ (50%), indicating that the reaction is agnostic to the halogen starting on the Co(III)–X centers. Similarly, as mentioned above, KBr could be used to convert 1 to 2-BrPy (44% yield), further supporting the idea that halex reactions can be driven to produce different heteroaryl halides based on the exogenous metal halide salt employed (Supporting Information Section 5.1). Finally, a gas release study was conducted to rule out Cl_2 release during the reaction,⁴⁷ despite the Co(III) oxidation state being retained (Figure S63). When $\text{Co}_2\text{Cl}_4(\text{btdd})$ was heated to 90 °C in 1,4-dioxane for 16 h, the resulting solution did not contain dissolved Cl_2 and the MOF did not undergo a color change, ruling out the involvement of generated Cl_2 during the reaction (Figure S63). Taken together, these results strongly point to the reaction proceeding through an $\text{S}_{\text{N}}\text{Ar}$ mechanism. At this time, we cannot rule out that the reaction proceeds through a concerted $\text{S}_{\text{N}}\text{Ar}$ pathway instead of through a discrete Meisenheimer intermediate.⁶⁷

Due to their insolubility, MOFs offer an inherent advantage compared to molecular catalysts—recyclability. As such, reactions performed on large scale are less wasteful because the catalyst can be recovered, regenerated, and reused in subsequent reactions.^{68,69} To exemplify this, a gram-scale chlorination was performed (Figure 5a), affording 5a in a yield (60%) comparable to that of the small-scale reaction (54%). The MOF used in this reaction was collected, washed with water and MeOH to remove residual reactants, and reactivated under vacuum before being reused in subsequent gram-scale chlorination reactions. Three consecutive reactions with the same batch of MOF exhibit yields (60%, 66%, and 57%) comparable to those of the small-scale reaction (Figure 5a). After the final reaction, the collected MOF was found to be crystalline via PXRD but contaminated with residual KCl and KBr (Figure S70). The contaminants were removed by washing with water and MeOH, and the resulting crystalline sample of MOF demonstrates a BET surface area comparable to that of $\text{Co}_2\text{Br}_2\text{Cl}_2(\text{btdd})$ (1059 ± 35 m²/g) (Figures S71 and S72). These Co(III)–X MOFs represent the first recyclable catalysts for halex reactions.

As heterogeneous catalysts, MOFs are also prime candidates for reactions performed in continuous flow.⁴⁸ Heterogeneous catalysis in flow can result in increased yields and decreased reaction times due to the increased interfacial area and mass transfer compared to batch conditions, while also improving

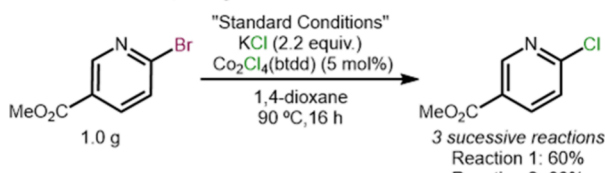
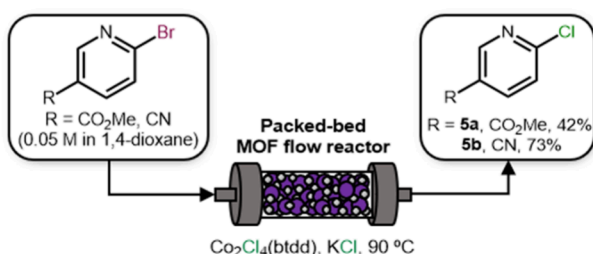
a Gram-scale, recyclable chlorination:**b** Chlorination in flow:

Figure 5. (a) Gram-scale, recyclable chlorination using $\text{Co}_2\text{Cl}_4(\text{btdd})$. (b) Chlorination in flow using a packed-bed-inspired MOF flow reactor packed with $\text{Co}_2\text{Cl}_4(\text{btdd})$ and KCl.

catalyst lifetimes and enabling catalyst recovery by combining reagent/catalyst separation with the reaction step.⁴⁹ By using a simple packed-bed flow reactor loaded with MOF and KCl (Figure S69), **5a** and **5b** can both be prepared from their corresponding heteroaryl bromides in comparable yields (42% and 73%, respectively) on a similar time scale (16 h) and at a similar temperature (90 °C) to batch reactions (Figure 5b).

CONCLUSION

In summary, we have demonstrated the first example of a MOF-catalyzed halex, a reaction that can be adapted to function in continuous flow. A novel MOF synthesis, used to prepare gram-scale batches of MOFs, was developed to streamline reaction development. Both halogenation reactions reported herein are milder than reported halex reactions using simple metal halide salts, and both show high tolerance for a range of pharmaceutically relevant heterocyclic systems and functional groups. As a result, this transformation represents a significant advance in the use of MOFs to catalyze reactions relevant to medicinal chemistry, an emerging application for these powerful materials.^{70,71} Although herein we focus on the fluorination and chlorination of heteroaryl bromides, this MOF platform can theoretically be used to drive other pharmaceutically relevant nucleophilic transformations, which we will explore in future work.

ASSOCIATED CONTENT

Supporting Information

The Supporting Information is available free of charge at <https://pubs.acs.org/doi/10.1021/jacs.3c13872>.

All synthetic procedures and characterization data (PDF)

AUTHOR INFORMATION

Corresponding Author

Phillip J. Milner – Department of Chemistry and Chemical Biology, Cornell University, Ithaca, New York 14850, United States; orcid.org/0000-0002-2618-013X;
Email: pjm347@cornell.edu

Author

Tyler J. Azbell – Department of Chemistry and Chemical Biology, Cornell University, Ithaca, New York 14850, United States

Complete contact information is available at:

<https://pubs.acs.org/10.1021/jacs.3c13872>

Funding

The development of MOF-driven catalytic halogen exchange was supported by the National Institute of General Medical Sciences of the National Institutes of Health under award number R35GM138165 (T.J.A., P.J.M.). The content is solely the responsibility of the authors and does not necessarily represent the official views of the National Institutes of Health. We acknowledge the support of a Camille Dreyfus Teacher-Scholar Award to P.J.M (TC-23-048). This work made use of the Cornell Center for Materials Research Shared Facilities, which are supported through the NSF MRSEC program (DMR-1719875). ^1H NMR data were collected on a Bruker INOVA 500 MHz spectrometer and a Bruker INOVA 400 MHz spectrometer that was purchased with support from the National Science Foundation (CHE-1531632).

Notes

The authors declare the following competing financial interest(s): P.J.M. is listed as a co-inventor on several patents related to MOFs.

ACKNOWLEDGMENTS

We thank Justin S. K. Ho (Cornell University) for his help in designing and machining the flow reactor. We thank Nicholas P. Bigham (Cornell University) and Prof. Justin J. Wilson for assistance with GFAAS. We thank Dr. Colin Gould (Princeton University) for assistance with interpreting SQUID magnetization data. We are grateful to Kaitlyn T. Keasler, Tristan A. Pitt, and Ronald T. Jerozal (Cornell University) for helpful discussions and assistance with the preparation of this manuscript.

REFERENCES

- Gillis, E. P.; Eastman, K. J.; Hill, M. D.; Donnelly, D. J.; Meanwell, N. A. Applications of Fluorine in Medicinal Chemistry. *J. Med. Chem.* **2015**, 58 (21), 8315–8359.
- Fauvarque, J. The Chlorine Industry. *Pure Appl. Chem.* **1996**, 68 (9), 1713–1720.
- Jeschke, P. Manufacturing Approaches of New Halogenated Agrochemicals. *Eur. J. Org. Chem.* **2022**, 2022 (12), No. e202101513.
- Ogawa, Y.; Tokunaga, E.; Kobayashi, O.; Hirai, K.; Shibata, N. Current Contributions of Organofluorine Compounds to the Agrochemical Industry. *iScience* **2020**, 23 (9), 101467.
- Chiodi, D.; Ishihara, Y. "Magic Chloro": Profound Effects of the Chlorine Atom in Drug Discovery. *J. Med. Chem.* **2023**, 66 (8), 5305–5331.
- Inoue, M.; Sumii, Y.; Shibata, N. Contribution of Organofluorine Compounds to Pharmaceuticals. *ACS Omega* **2020**, 5 (19), 10633–10640.
- Ni, C.; Hu, J. The Unique Fluorine Effects in Organic Reactions: Recent Facts and Insights into Fluoroalkylations. *Chem. Soc. Rev.* **2016**, 45 (20), 5441–5454.
- Keam, S. J. Piflufolastat F 18: Diagnostic First Approval. *Molecular Diagnosis & Therapy* **2021**, 25 (5), 647–656.
- Voter, A. F.; Werner, R. A.; Pienta, K. J.; Gorin, M. A.; Pomper, M. G.; Solnes, L. B.; Rowe, S. P. Piflufolastat F-18 (^{18}F -DCFPyL) for PSMA PET Imaging in Prostate Cancer. *Expert Review of Anticancer Therapy* **2022**, 22 (7), 681–694.

- (10) Spande, T. F.; Garraffo, H. M.; Edwards, M. W.; Yeh, H. J. C.; Pannell, L.; Daly, J. W. Epibatidine: A Novel (Chloropyridyl)-Azabicycloheptane with Potent Analgesic Activity from an Ecuadorian Poison Frog. *J. Am. Chem. Soc.* **1992**, *114* (9), 3475–3478.
- (11) Vitaku, E.; Smith, D. T.; Njardarson, J. T. Analysis of the Structural Diversity, Substitution Patterns, and Frequency of Nitrogen Heterocycles among U.S. FDA Approved Pharmaceuticals. *J. Med. Chem.* **2014**, *57* (24), 10257–10274.
- (12) Kosjek, T.; Heath, E. Halogenated Heterocycles as Pharmaceuticals. In *Halogenated Heterocycles: Synthesis, Application and Environment*; Iskra, J., Ed.; Springer: Berlin, 2012; pp 219–246.
- (13) Carboni, J. M.; Wittman, M.; Yang, Z.; Lee, F.; Greer, A.; Hurlburt, W.; Hillerman, S.; Cao, C.; Cantor, G. H.; Dell-John, J.; Chen, C.; Discenzo, L.; Menard, K.; Li, A.; Trainor, G.; Vyas, D.; Kramer, R.; Attar, R. M.; Gottardis, M. M. BMS-754807, a Small Molecule Inhibitor of Insulin-like Growth Factor-1R/IR. *Molecular Cancer Therapeutics* **2009**, *8* (12), 3341–3349.
- (14) Wittman, M. D.; Carboni, J. M.; Yang, Z.; Lee, F. Y.; Antman, M.; Attar, R.; Balimane, P.; Chang, C.; Chen, C.; Discenzo, L.; Frennesson, D.; Gottardis, M. M.; Greer, A.; Hurlburt, W.; Johnson, W.; Langley, D. R.; Li, A.; Li, J.; Liu, P.; Mastalerz, H.; Mathur, A.; Menard, K.; Patel, K.; Sack, J.; Sang, X.; Saulnier, M.; Smith, D.; Stefanski, K.; Trainor, G.; Velaparthi, U.; Zhang, G.; Zimmermann, K.; Vyas, D. M. Discovery of a 2,4-Disubstituted Pyrrolo[1,2-f][1,2,4]Triazine Inhibitor (BMS-754807) of Insulin-like Growth Factor Receptor (IGF-1R) Kinase in Clinical Development. *J. Med. Chem.* **2009**, *52* (23), 7360–7363.
- (15) Salehi, B.; Sestito, S.; Rapposelli, S.; Peron, G.; Calina, D.; Sharifi-Rad, M.; Sharopov, F.; Martins, N.; Sharifi-Rad, J. Epibatidine: A Promising Natural Alkaloid in Health. *Biomolecules* **2019**, *9* (1), 6.
- (16) Caron, S. Where Does the Fluorine Come From? A Review on the Challenges Associated with the Synthesis of Organofluorine Compounds. *Org. Process Res. Dev.* **2020**, *24* (4), 470–480.
- (17) Van Der Puy, M. Direct Fluorination of Substituted Pyridines. *Tetrahedron Lett.* **1987**, *28* (3), 255–258.
- (18) King, J. F.; Hawson, A.; Huston, B. L.; Danks, L. J.; Komery, J. Chlorination of Heterocyclic and Acyclic Sulfonhydrazones. *Can. J. Chem.* **1971**, *49* (6), 943–955.
- (19) Roe, A. Preparation of Aromatic Fluorine Compounds from Diazonium Fluoroborates. *Organic Reactions* **2011**, *193*–228.
- (20) Cresswell, A. J.; Davies, S. G.; Roberts, P. M.; Thomson, J. E. Beyond the Balz-Schiemann Reaction: The Utility of Tetrafluoroborates and Boron Trifluoride as Nucleophilic Fluoride Sources. *Chem. Rev.* **2015**, *115* (2), 566–611.
- (21) Campbell, M. G.; Ritter, T. Modern Carbon-Fluorine Bond Forming Reactions for Aryl Fluoride Synthesis. *Chem. Rev.* **2015**, *115* (2), 612–633.
- (22) Adams, D. J.; Clark, J. H. Nucleophilic Routes to Selectively Fluorinated Aromatics. *Chem. Soc. Rev.* **1999**, *28* (4), 225–231.
- (23) Furuya, T.; Klein, J.; Ritter, T. Carbon-Fluorine Bond Formation for the Synthesis of Aryl Fluorides. *Synthesis* **2010**, *2010* (11), 1804–1821.
- (24) Pleschke, A.; Marhold, A.; Schneider, M.; Kolomeitsev, A.; Röschenthaler, G.-V. Halex Reactions of Aromatic Compounds Catalysed by 2-Azaallenium, Carbophosphazinium, Aminophosphonium and Diphosphazinium Salts: A Comparative Study. *J. Fluor. Chem.* **2004**, *125* (6), 1031–1038.
- (25) Allen, L. J.; Muhuhi, J. M.; Bland, D. C.; Merzel, R.; Sanford, M. S. Mild Fluorination of Chloropyridines with in Situ Generated Anhydrous Tetrabutylammonium Fluoride. *J. Org. Chem.* **2014**, *79* (12), 5827–5833.
- (26) Schimler, S. D.; Ryan, S. J.; Bland, D. C.; Anderson, J. E.; Sanford, M. S. Anhydrous Tetramethylammonium Fluoride for Room-Temperature S_NAr Fluorination. *J. Org. Chem.* **2015**, *80* (24), 12137–12145.
- (27) Morales-Colón, M. T.; See, Y. Y.; Lee, S. J.; Scott, P. J. H.; Bland, D. C.; Sanford, M. S. Tetramethylammonium Fluoride Alcohol Adducts for S_NAr Fluorination. *Org. Lett.* **2021**, *23* (11), 4493–4498.
- (28) Sun, H.; DiMango, S. G. Anhydrous Tetrabutylammonium Fluoride. *J. Am. Chem. Soc.* **2005**, *127* (7), 2050–2051.
- (29) Ryan, S. J.; Schimler, S. D.; Bland, D. C.; Sanford, M. S. Acyl Azolium Fluorides for Room Temperature Nucleophilic Aromatic Fluorination of Chloro- and Nitroarenes. *Org. Lett.* **2015**, *17* (8), 1866–1869.
- (30) Wallenfels, K.; Friedrich, K. Synthese von Tetracyan-m-Xylo, Pentacyanoluol Und Hexacyanbenzol. *Tetrahedron Lett.* **1963**, *4* (19), 1223–1227.
- (31) Neumann, C. N.; Ritter, T. Transition-Metal-Mediated and Transition-Metal-Catalyzed Carbon-Fluorine Bond Formation. *Organic Reactions* **2020**, *1*–181.
- (32) Klapars, A.; Buchwald, S. L. Copper-Catalyzed Halogen Exchange in Aryl Halides: An Aromatic Finkelstein Reaction. *J. Am. Chem. Soc.* **2002**, *124* (50), 14844–14845.
- (33) Grushin, V. V. The Organometallic Fluorine Chemistry of Palladium and Rhodium: Studies toward Aromatic Fluorination. *Acc. Chem. Res.* **2010**, *43* (1), 160–171.
- (34) Sather, A. C.; Buchwald, S. L. The Evolution of Pd⁰/Pd^{II}-Catalyzed Aromatic Fluorination. *Acc. Chem. Res.* **2016**, *49* (10), 2146–2157.
- (35) Hollingworth, C.; Gouverneur, V. Transition Metal Catalysis and Nucleophilic Fluorination. *Chem. Commun.* **2012**, *48* (24), 2929–2942.
- (36) Yang, S. H.; Li, C. S.; Cheng, C. H. Halide Exchange Reactions between Aryl Halides and Alkali Halides Catalyzed by Nickel Metal. *J. Org. Chem.* **1987**, *52* (4), 691–694.
- (37) Casitas, A.; Canta, M.; Solà, M.; Costas, M.; Ribas, X. Nucleophilic Aryl Fluorination and Aryl Halide Exchange Mediated by a Cu^I/Cu^{III} Catalytic Cycle. *J. Am. Chem. Soc.* **2011**, *133* (48), 19386–19392.
- (38) Fier, P. S.; Hartwig, J. F. Copper-Mediated Fluorination of Aryl Iodides. *J. Am. Chem. Soc.* **2012**, *134* (26), 10795–10798.
- (39) Vladimir Grushin. Processes for Preparing Fluoroarenes from Haloarenes. US 7202338B2. <https://patents.google.com/patent/US7202338B2/en>.
- (40) Grushin, V. V. Palladium Fluoride Complexes: One More Step toward Metal-Mediated C-F Bond Formation. *Chem.—Eur. J.* **2002**, *8* (5), 1006–1014.
- (41) Campbell, M. G.; Hoover, A. J.; Ritter, T. Transition Metal-Mediated and Metal-Catalyzed Carbon-Fluorine Bond Formation. In *Organometallic Fluorine Chemistry*; Braun, T., Hughes, R. P., Eds.; Springer International Publishing: Cham, 2015; pp 1–53.
- (42) Thathagar, M. B.; Rothenberg, G. One-Pot Pd/C Catalysed 'Domino' HALEX and Sonogashira Reactions: A Ligand- and Cu-Free Alternative. *Org. Biomol. Chem.* **2006**, *4* (1), 111–115.
- (43) Leclerc, M. C.; Bayne, J. M.; Lee, G. M.; Gorelsky, S. I.; Vasiliu, M.; Korobkov, I.; Harrison, D. J.; Dixon, D. A.; Baker, R. T. Perfluoroalkyl Cobalt(III) Fluoride and Bis(Perfluoroalkyl) Complexes: Catalytic Fluorination and Selective Difluorocarbene Formation. *J. Am. Chem. Soc.* **2015**, *137* (51), 16064–16073.
- (44) Cozzolino, A. F.; Brozek, C. K.; Palmer, R. D.; Yano, J.; Li, M.; Dincă, M. Ligand Redox Non-Innocence in the Stoichiometric Oxidation of Mn₂(2,5-Dioxidoterephthalate) (Mn-MOF-74). *J. Am. Chem. Soc.* **2014**, *136* (9), 3334–3337.
- (45) Jaramillo, D. E.; Reed, D. A.; Jiang, H. Z. H.; Oktawiec, J.; Mara, M. W.; Forse, A. C.; Lussier, D. J.; Murphy, R. A.; Cunningham, M.; Colombo, V.; Shuh, D. K.; Reimer, J. A.; Long, J. R. Selective Nitrogen Adsorption via Backbonding in a Metal-Organic Framework with Exposed Vanadium Sites. *Nat. Mater.* **2020**, *19* (5), 517–521.
- (46) Azbell, T. J.; Pitt, T. A.; Bollmeyer, M. M.; Cong, C.; Lancaster, K. M.; Milner, P. J. Ionothermal Synthesis of Metal-Organic Frameworks Using Low-Melting Metal Salt Precursors. *Angew. Chem., Int. Ed.* **2023**, *62* (17), No. e202218252.
- (47) Tulchinsky, Y.; Hendon, C. H.; Lomachenko, K. A.; Borfecchia, E.; Melot, B. C.; Hudson, M. R.; Tarver, J. D.; Korzyński, M. D.; Stubbs, A. W.; Kagan, J. J.; Lamberti, C.; Brown, C. M.; Dincă, M. Reversible Capture and Release of Cl₂ and Br₂ with a Redox-Active

- Metal-Organic Framework. *J. Am. Chem. Soc.* **2017**, *139* (16), 5992–5997.
- (48) Rieth, A. J.; Tulchinsky, Y.; Dincă, M. High and Reversible Ammonia Uptake in Mesoporous Azolate Metal-Organic Frameworks with Open Mn, Co, and Ni Sites. *J. Am. Chem. Soc.* **2016**, *138* (30), 9401–9404.
- (49) Plutschack, M. B.; Pieber, B.; Gilmore, K.; Seeberger, P. H. The Hitchhiker's Guide to Flow Chemistry. *Chem. Rev.* **2017**, *117* (18), 11796–11893.
- (50) Langlois, B.; Gilbert, L.; Forat, G. Fluorination of Aromatic Compounds by Halogen Exchange with Fluoride Anions (“Halex” Reaction). In *Industrial Chemistry Library*; Desmurs, J.-R., Ratton, S., Eds.; Elsevier: 1996; Vol. 8, pp 244–292.
- (51) Jerozal, R. T.; Pitt, T. A.; MacMillan, S. N.; Milner, P. J. High-Concentration Self-Assembly of Zirconium- and Hafnium-Based Metal-Organic Materials. *J. Am. Chem. Soc.* **2023**, *145* (24), 13273–13283.
- (52) Sarie, J. C.; Thiehoff, C.; Mudd, R. J.; Daniliuc, C. G.; Kehr, G.; Gilmour, R. Deconstructing the Catalytic, Vicinal Difluorination of Alkenes: HF-Free Synthesis and Structural Study of p-TolIF₂. *J. Org. Chem.* **2017**, *82* (22), 11792–11798.
- (53) Lesniewski, J. E.; Zheng, K.; Lecchi, P.; Dain, D.; Jorabchi, K. High-Sensitivity Elemental Mass Spectrometry of Fluorine by Ionization in Plasma Afterglow. *Anal. Chem.* **2019**, *91* (6), 3773–3777.
- (54) Wang, Y.; Huang, N.-Y.; Shen, J.-Q.; Liao, P.-Q.; Chen, X.-M.; Zhang, J.-P. Hydroxide Ligands Cooperate with Catalytic Centers in Metal-Organic Frameworks for Efficient Photocatalytic CO₂ Reduction. *J. Am. Chem. Soc.* **2018**, *140* (1), 38–41.
- (55) Rieth, A. J.; Wright, A. M.; Skorupskii, G.; Mancuso, J. L.; Hendon, C. H.; Dincă, M. Record-Setting Sorbents for Reversible Water Uptake by Systematic Anion Exchanges in Metal-Organic Frameworks. *J. Am. Chem. Soc.* **2019**, *141* (35), 13858–13866.
- (56) Oppenheim, J. J.; Mancuso, J. L.; Wright, A. M.; Rieth, A. J.; Hendon, C. H.; Dincă, M. Divergent Adsorption Behavior Controlled by Primary Coordination Sphere Anions in the Metal-Organic Framework Ni₂X₂BTDD. *J. Am. Chem. Soc.* **2021**, *143* (40), 16343–16347.
- (57) Paparella, A. S.; Lee, K. J.; Hayes, A. J.; Feng, J.; Feng, Z.; Cini, D.; Deshmukh, S.; Booker, G. W.; Wilce, M. C. J.; Polyak, S. W.; Abell, A. D. Halogenation of Biotin Protein Ligase Inhibitors Improves Whole Cell Activity against *Staphylococcus Aureus*. *ACS Infect. Dis.* **2018**, *4* (2), 175–184.
- (58) Laxio Arenas, J.; Retailleau, P.; Gillet, J.-M.; Ghermani, N.-E.; Ongeri, S.; Crousse, B. 5-Fluoro-1,2,3-Triazole Motif in Peptides and Its Electronic Properties. *Org. Biomol. Chem.* **2022**, *20* (43), 8410–8414.
- (59) Worrell, B. T.; Hein, J. E.; Fokin, V. V. Halogen Exchange (Halex) Reaction of 5-Iodo-1,2,3-Triazoles: Synthesis and Applications of 5-Fluorotriazoles. *Angew. Chem., Int. Ed.* **2012**, *51* (47), 11791–11794.
- (60) Silva, S. L.; Valle, M. S.; Pliego, J. R. Micro-Solvation and Counter Ion Effects on Ionic Reactions: Activation of Potassium Fluoride with 18-Crown-6 and Tert-Butanol in Aprotic Solvents. *J. Mol. Liq.* **2020**, *319*, 114211.
- (61) Milner, P. J.; Yang, Y.; Buchwald, S. L. In-Depth Assessment of the Palladium-Catalyzed Fluorination of Five-Membered Heteroaryl Bromides. *Organometallics* **2015**, *34* (19), 4775–4780.
- (62) Frontmatter. In *Category 2, Hetarenes and Related Ring Systems*; Science of Synthesis; Georg Thieme Verlag KG: Stuttgart, 2015; Vol. 12.
- (63) Wang, W.; Huo, T.; Zhao, X.; Qin, Q.; Liang, Y.; Song, S.; Liu, G.; Jiao, N. Nitromethane-Enabled Fluorination of Styrenes and Arenes. *CCS Chem.* **2020**, *2* (6), 566–575.
- (64) Siméon, F. G.; Wendahl, M. T.; Pike, V. W. The [¹⁸F]2-Fluoro-1,3-Thiazolyl Moiety—an Easily-Accessible Structural Motif for Prospective Molecular Imaging Radiotracers. *Tetrahedron Lett.* **2010**, *51* (46), 6034–6036.
- (65) Yu, L.; Deng, M.; Wang, N.; Xiang, G. The New Convenient Synthesis of 6-Fluoropurine and Its 7-/9-Unsubstituted Analogues. *Heterocycles* **2012**, *85* (12), 2999–3006.
- (66) Meisenheimer Complex. In *Name Reactions: A Collection of Detailed Reaction Mechanisms*; Li, J. J., Ed.; Springer: Berlin, 2006; pp 371–372.
- (67) Kwan, E. E.; Zeng, Y.; Besser, H. A.; Jacobsen, E. N. Concerted Nucleophilic Aromatic Substitutions. *Nat. Chem.* **2018**, *10* (9), 917–923.
- (68) Thomas, J. M.; Raja, R. The Advantages and Future Potential of Single-Site Heterogeneous Catalysts. *Top. Catal.* **2006**, *40* (1), 3–17.
- (69) Chatterjee, A.; Hu, X.; Lam, F. L.-Y. Towards a Recyclable MOF Catalyst for Efficient Production of Furfural. *Catal. Today* **2018**, *314*, 129–136.
- (70) Ahmad, B. I. Z.; Keasler, K. T.; Stacy, E. E.; Meng, S.; Hicks, T. J.; Milner, P. J. MOFganic Chemistry: Challenges and Opportunities for Metal-Organic Frameworks in Synthetic Organic Chemistry. *Chem. Mater.* **2023**, *35* (13), 4883–4896.
- (71) Pascanu, V.; González Miera, G.; Inge, A. K.; Martín-Matute, B. Metal-Organic Frameworks as Catalysts for Organic Synthesis: A Critical Perspective. *J. Am. Chem. Soc.* **2019**, *141* (18), 7223–7234.